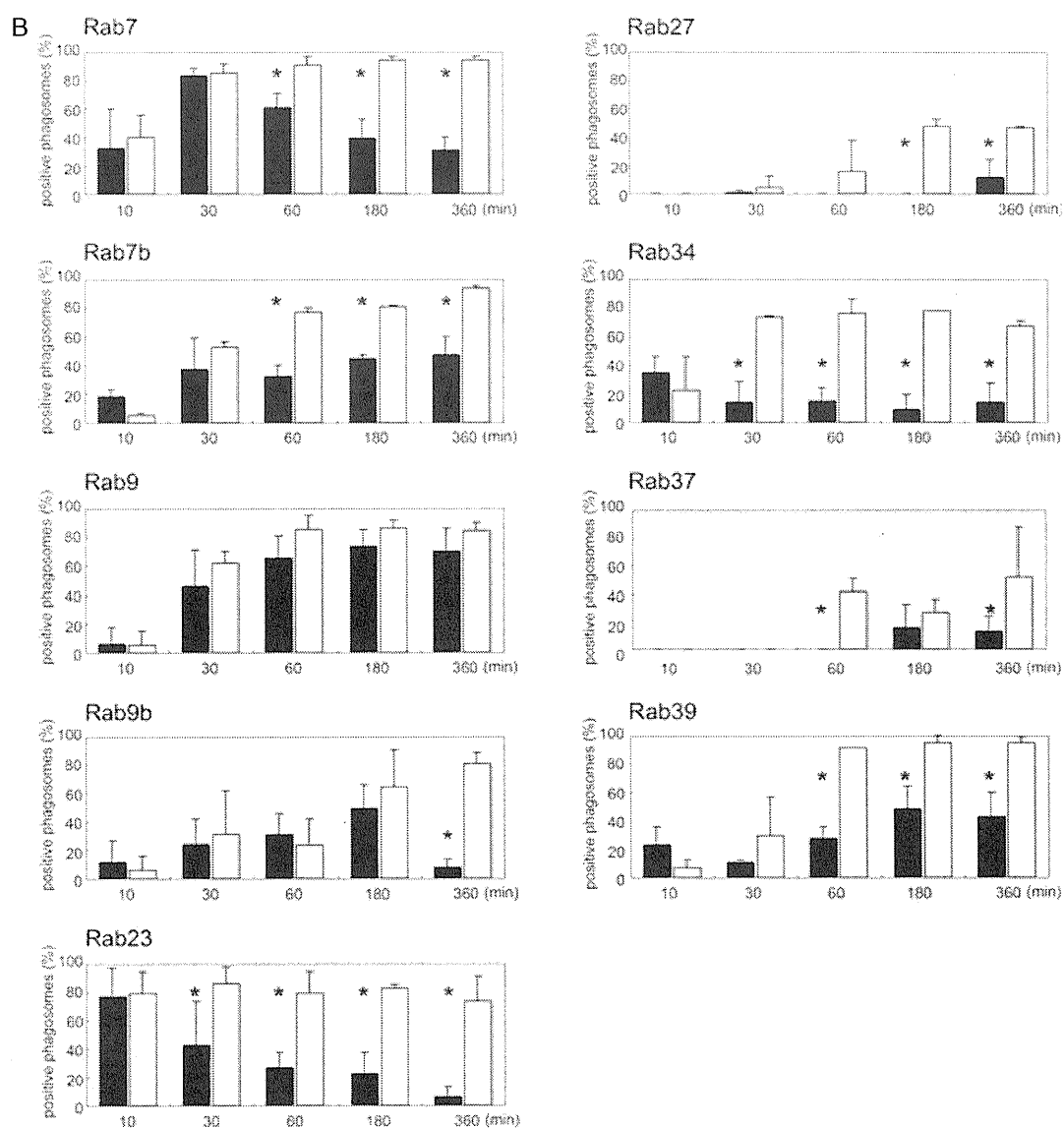


**Figure 2: Localization kinetics of Rab GTPases on *M. tb*- and *S. aureus*-containing phagosomes.** The proportions of Rab GTPase-positive phagosomes containing *M. tb* and *S. aureus* were examined at the indicated time-points p.i. Data represent the means and standard deviations of three independent experiments in which more than 100 phagosomes were counted for each condition. Rab GTPases were classified into two types according to their localization on *S. aureus*-containing phagosomes as follows: (A) Rab GTPases transiently localizing to the phagosomes and (B) Rab GTPases consecutively or accumulatively localizing to the phagosomes. Black and white bars indicate the proportion of Rab-positive phagosomes containing *M. tb* and *S. aureus*, respectively. \*p < 0.05 (unpaired Student's t-test).

## Localization of Rab GTPases on *M. tb*-Containing Phagosomes



**Figure 2:** *Continued.*

*M. tb* for 2 or 8 h. Phagosomal fractions were isolated as previously reported (26,27). We confirmed that the phagosomal fractions were not contaminated with other subcellular organelles using electron microscopy (Figure 3A) as shown previously (17). Immunoblotting analysis revealed that Rab5, Rab7, Rab9, Rab14 and Rab22a were recruited to both phagosomal fractions (Figure 3B). We quantified the band intensities corresponding to Rab GTPases in latex bead- and *M. tb*-containing phagosomal fractions at 2 and 8 h p.i. to follow the dynamics of Rab GTPases on the phagosomes (Figure 3C). In the latex bead-containing phagosomes, the amounts of Rab5, Rab7, Rab9 and Rab22a at 8 h showed no change or slightly decreased in comparison with those at 2 h, whereas the amount of Rab14 at 8 h decreased significantly to about 30% of that at 2 h. In *M. tb* phagosomal fractions, the amounts

of Rab5, Rab7, Rab14 and Rab22a at 8 h demonstrated significant decreases to about 40, 20, 60 and 30% of those at 2 h, respectively. Rab9 did not show significant changes in *M. tb* phagosomal fractions. These results suggest that Rab5, Rab7, Rab9 and Rab22a are associated with the latex bead-containing phagosomes, but these Rab GTPases except for Rab9 are subsequently released from *M. tb*-containing phagosomes, and that recruited Rab14 is dissociated from both phagosomes.

### **A network of Rab GTPases regulating phagosome maturation**

To examine the contribution of 22 Rab GTPases localizing to *S. aureus*-containing phagosomes during phagosome maturation, Raw264.7 macrophages were transfected with two expression plasmids for EGFP and the

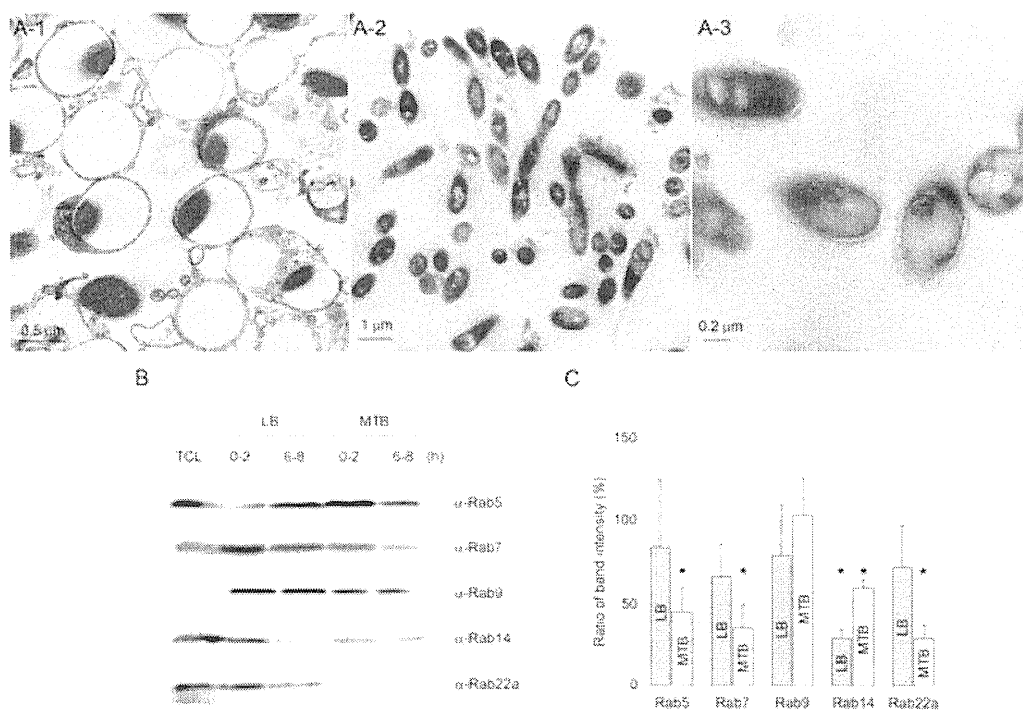


**Figure 3: Rab GTPases localization in isolated *M. tb* phagosomal fractions.** A) Thin-section electron micrographs of isolated phagosomal fractions containing the latex beads (A-1) and *M. tb* (A-2, A-3) for 6 h. B) Immunoblotting analysis of latex bead and *M. tb* phagosomal fractions with antibodies to Rab5, Rab7, Rab9, Rab14 and Rab22a is shown. Latex beads (LB) or *M. tb* (MTB) were internalized for 2 h and phagosomal fractions were collected immediately (0–2 h) or after further incubation for 6 h (6–8 h). Total cell lysates from Raw264.7 (TCL) and phagosomal fractions were subjected to SDS–PAGE, followed by immunoblotting analysis using the indicated antibodies. C) Ratios of band intensity for Rab GTPase at 6–8 h relative to that at 0–2 h in phagosomal fractions. Gray and white bars show the ratio of band intensity of indicated Rab at 6–8 h as compared to that at 0–2 h in latex bead and *M. tb* phagosomal fractions, respectively. Data represent the means and standard deviations of three independent experiments. \* $p < 0.05$  (paired Student's *t*-test).

dominant-negative (DN) form of each Rab gene. For the evaluation of phagosome maturation, we determined the degree of phagosomal acidification and the recruitment of cathepsin D to the phagosome, because both events were exceedingly inhibited in the phagosomes containing *M. tb* H37Rv in macrophages (Figure 1). Transfected cells were allowed to phagocytose latex beads for 3 h, then acidification of the phagosome was investigated (Figure 4). Phagocytosing cells were stained with LysoTracker and its accumulation within phagosomes was observed by LSCM. Phagosomal acidification was clearly observed in control cells (Figure 4A). We found that phagosomal acidification was inhibited by Rab7DN as described previously (5), confirming that the experiment was being conducted correctly. Expression of Rab20DN or Rab39DN also inhibited the accumulation of LysoTracker within the phagosomes (Figure 4B,C). We quantified the fluorescent density of LysoTracker accumulated in phagosomes relative to that in other endosomal/lysosomal (E/L) components of transfected cells expressing DN forms of Rab GTPases (Figure 4D). As expected, the expression of Rab7DN, Rab20DN and Rab39DN decreased the fluorescent ratio in comparison with that in the control cells. These results suggest that Rab7, Rab20 and Rab39

function in phagosomal acidification. The mean fluorescence intensities derived from LysoTracker staining were not affected by the expression of Rab7DN, Rab20DN or Rab39DN (Figure S3), indicating that expression of these DN forms of Rab GTPases had no effect on the generation of acidic vacuoles in macrophages.

We next examined the recruitment of cathepsin D to the phagosomes in macrophages expressing DN forms of the Rab GTPases (Figure 5). Transfected cells were allowed to phagocytose latex beads for 3 h and were then stained with an anti-cathepsin D antibody. Stained cells were observed by LSCM. Cathepsin D was recruited to the phagosome in the control cells (Figure 5A). The recruitment of cathepsin D was inhibited by the expression of Rab7DN as described previously (17). Immunofluorescence microscopy also demonstrated that the expression of Rab20DN, Rab22bDN, Rab32DN, Rab34DN, Rab38DN or Rab43DN inhibited the recruitment of cathepsin D to the phagosomes (Figure 5B,C). The ratiometric quantification revealed that the expression of these DN forms of Rab GTPases decreased the association of cathepsin D with phagosomes (Figure 5D). Immunoblotting analysis revealed that the amount of products and the processing

## Localization of Rab GTPases on *M. tb*-Containing Phagosomes

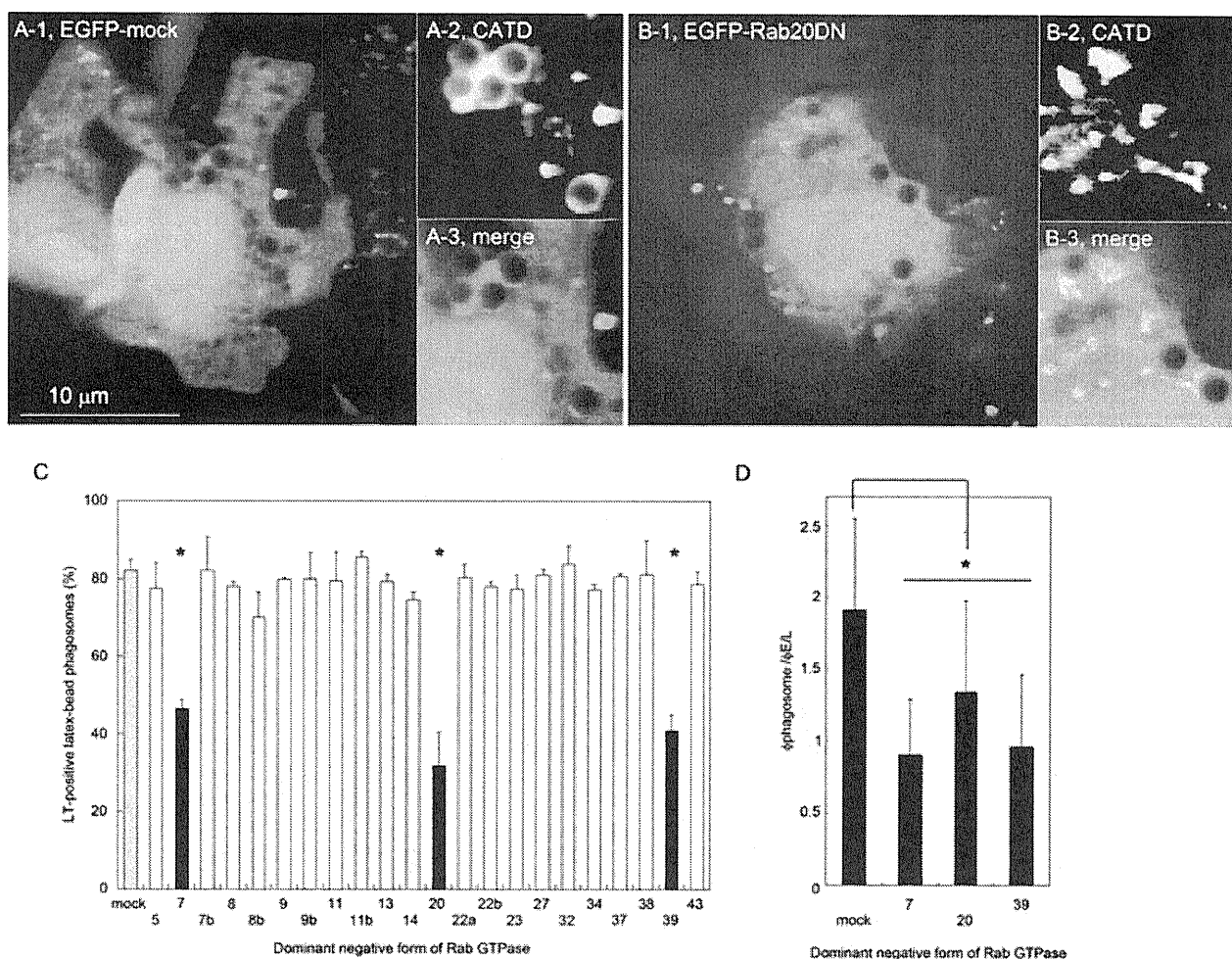


**Figure 4: Phagosomal acidification in macrophages expressing the DN forms of Rab GTPases.** Raw264.7 macrophages were transfected with plasmids encoding EGFP and control vector (mock) (A) or the DN form of Rab20 (Rab20DN) (B). Transfected cells were allowed to phagocytose latex beads for 3 h and were then stained with LysoTracker (LT). Stained cells were observed by LSM. Enlarged images of the latex bead-containing phagosomes in A-1 and B-1 are represented in A-2, A-3 and B-2, B-3, respectively. C) The proportion of LysoTracker-positive phagosomes in macrophages expressing the DN forms of Rab GTPases. Data represent the means and standard deviations of three independent experiments in which more than 100 phagosomes were counted for each condition. D) Ratiometric quantification of fluorescent density of LysoTracker associated with the phagosomes ( $\phi$ phagosome) relative to that of other  $\phi$ E/L components. Data represent the means and standard deviations of three independent experiments in which more than 100 phagosomes were examined for each condition. \* $p < 0.05$  (unpaired Student's *t*-test).

of cathepsin D did not change significantly in the cells expressing the DN forms of the Rab GTPases as compared with the control cells (data not shown). These results suggest that Rab7, Rab20, Rab22b, Rab32, Rab34, Rab38 and Rab43 regulate the recruitment of cathepsin D to the phagosomes.

### Constitutively active forms of Rab GTPases were dissociated from *M. tb*-containing phagosomes

To elucidate the mechanism by which Rab GTPases are dissociated from *M. tb*-containing phagosomes, we examined the localization of the constitutively active (CA) forms of Rab GTPases regulating phagosome maturation on *M. tb*-containing phagosomes. We previously

demonstrated that Rab7CA is released from *M. tb*-containing phagosomes (17). In this study, we found that the recruitment of Rab20CA, Rab32CA, Rab34CA, Rab38CA and Rab39CA to *M. tb*-containing phagosomes is also impaired, in a similar way to the wild-type versions of these Rab GTPases (data not shown). We next examined the fusion of *M. tb*-containing phagosomes with lysosomes in macrophages expressing the CA forms of the Rab GTPases (Figure 6). Macrophages transfected with the expression plasmids for EGFP and each CA of Rab GTPase were preloaded with Texas Red-dextran and then infected with Alexa405-fluorophore-labeled *M. tb* for 6 h. Lysosomes did not fuse with the phagosomes containing live *M. tb* in macrophages expressing Rab7CA, Rab20CA, Rab32CA, Rab34CA, Rab38CA or Rab39CA

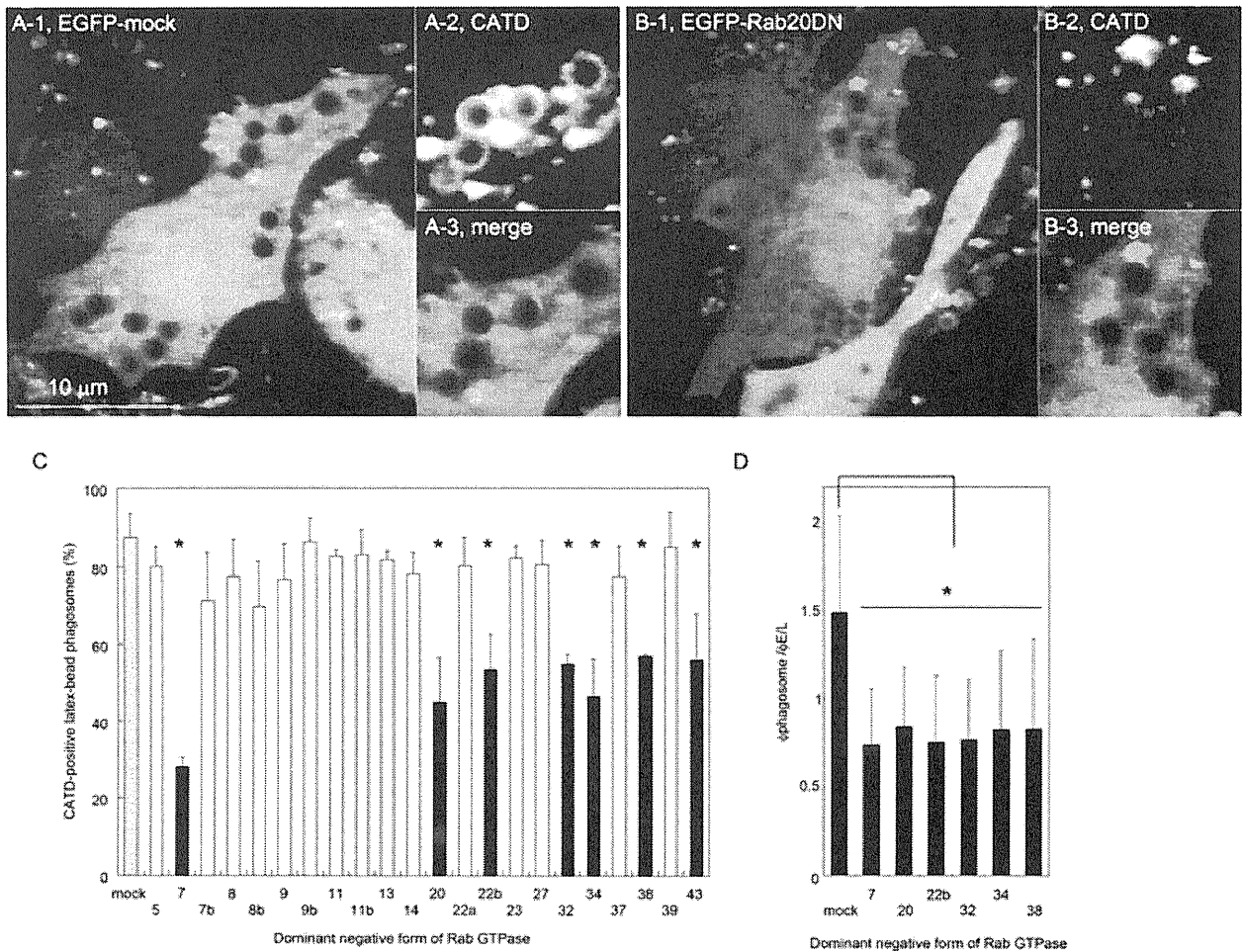


**Figure 5: Cathepsin D recruitment to phagosomes in macrophages expressing the DN form of Rab GTPases.** Raw264.7 macrophages were transfected with plasmids encoding EGFP and control vector (mock) (A) or Rab20DN (B). Transfected cells were allowed to phagocytose latex beads for 3 h and were then stained with anti-cathepsin D (CATD) and Alexa568-conjugated secondary antibodies. Stained cells were observed by LSCM. Enlarged images of the latex bead-containing phagosomes in A-1 and B-1 are represented in A-2, A-3 and B-2, B-3, respectively. C) The proportion of cathepsin D-positive phagosomes in macrophages expressing the DN forms of Rab GTPases. Data represent the means of three independent experiments in which more than 100 phagosomes were counted for each condition. D) Ratiometric quantification of fluorescent density of cathepsin D associated with the phagosomes ( $\phi_{\text{phagosome}}$ ) relative to that of other  $\phi_{\text{E/L}}$  components. Data represent the means and standard deviations of three independent experiments in which more than 100 phagosomes were examined for each condition. \* $p < 0.05$  (unpaired Student's  $t$ -test).

(Figure 6 and data not shown). Taken together, these results suggest that these Rab GTPases are not directly targeted by *M. tb* for inhibition of phagolysosome biogenesis and suggest instead that the difference in the localization of Rab GTPases between *S. aureus*- and *M. tb*-containing phagosomes is due to difference in how the phagosomes change or evolve over time.

**Localization of Rab GTPases on phagosomes containing an avirulent *M. tb* strain**

To investigate the correlation between the dissociation of Rab GTPases and the arrest of phagosome maturation, we examined the localization of Rab GTPases on phagosomes containing an attenuated strain, *M. tb* H37Ra. The proliferative activity of *M. tb* H37Ra, within

infected macrophages was reduced compared with that of the virulent *M. tb* H37Rv strain (data not shown), suggesting that the inhibition of phagolysosome biogenesis was suppressed in macrophages infected with *M. tb* H37Ra. We examined the fusion of *M. tb* H37Ra phagosomes with lysosomes in infected macrophages. Raw264.7 macrophages were preloaded with Texas Red-dextran, infected with *M. tb* strain H37Ra for 6 h and then observed by LSCM. Stronger fluorescent signals derived from dextran were observed within the phagosomes containing *S. aureus*. The fluorescent signals on *M. tb* H37Ra phagosomes were weaker than those on *S. aureus*-containing phagosomes but stronger than those on *M. tb* H37Rv phagosomes (Figure 7A–D). These results suggest that *M. tb* H37Ra phagosomes have the intermediate

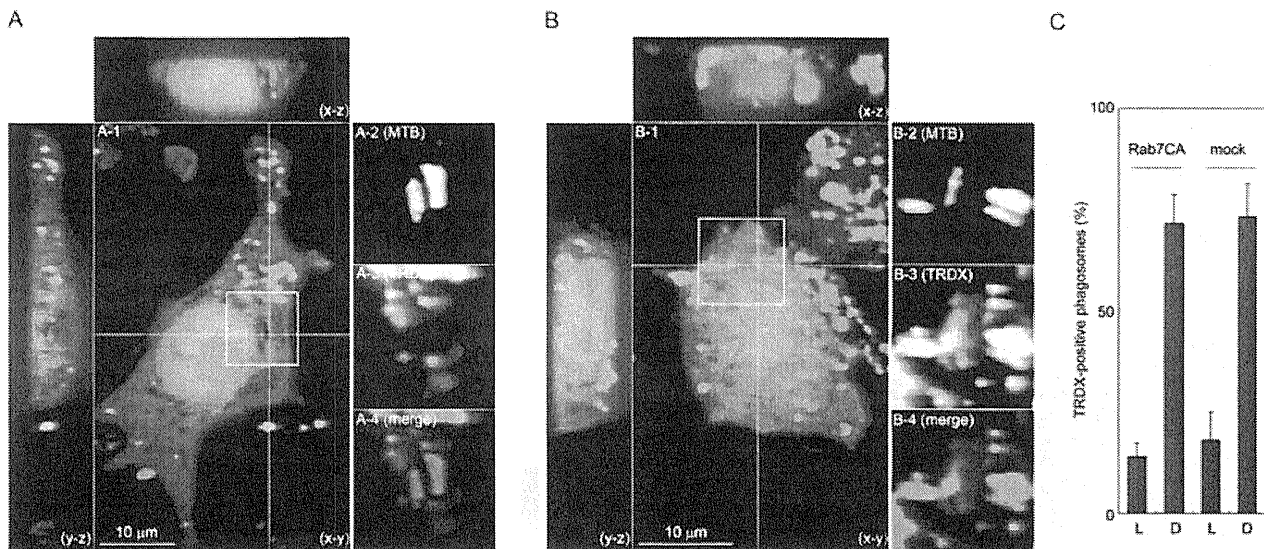


**Figure 6: Impairment of fusion of lysosomes with *M. tb*-containing phagosomes in macrophages expressing the CA form of Rab7.** Raw264.7 macrophages were transfected with plasmids expressing EGFP and the CA form of Rab7 (Rab7CA). Transfected cells were preloaded with Texas Red-dextran (TRDX) to label lysosomal vesicles, followed by incubation with live (A) and dead (B) *M. tb* labeled with Alexa405-fluorophore for 6 h. Fixed cells were observed by LSCM. Projections of focal planes with  $y-z$  and  $x-z$  side views show the sequestration and colocalization of fluorescent dextrans with *M. tb*-containing phagosomes in (A) and (B), respectively. Enlarged images showing the *M. tb*-containing phagosomes of A-1 are presented in A-2, A-3 and A-4. Enlarged images showing the *M. tb*-containing phagosomes of B-1 are shown in B-2, B-3 and B-4. A-2 and B-2 show live and dead *M. tb* (MTB), respectively. A-3 and B-3 show the localization of fluorescent dextran (TRDX). A-4 and B-4 show the merged images of macrophages and bacteria (merge). Scale bar, 10  $\mu\text{m}$ . C) The proportion of *M. tb*-containing phagosomes labeled with Texas Red-dextran in macrophages expressing Rab7CA. Macrophages transfected with the plasmid expressing Rab7CA or control vector (mock) were incubated with live (L) or dead (D) *M. tb* for 6 h. Data represent the means of three independent experiments in which more than 100 phagosomes were counted for each condition.

ability to fuse with lysosomal vesicles compared with *M. tb* H37Rv and *S. aureus*-containing phagosomes. We finally examined the association of Rab GTPases regulating phagosome maturation with phagosomes containing *M. tb* strain H37Ra. Macrophages expressing EGFP-Rab GTPases found to be involved in phagosome maturation were infected with Texas Red-labeled *M. tb* strain H37Ra or H37Rv for 6 h. The proportions of Rab7-, Rab20-, Rab34- and Rab39-positive phagosomes containing *M. tb* strain H37Ra were significantly higher than those of phagosomes containing *M. tb* strain H37Rv (Figure 7E), although those were lower than those of phagosomes containing *S. aureus* (Figure 2). These results suggest that *M. tb* strain H37Ra impairs the association of Rab GTPases regulating phagosome maturation to phagosomes, but less severely than *M. tb* strain H37Rv, leading to reduced fusion of lysosomal vesicles with phagosomes.

## Discussion

Intracellular pathogens are known to disrupt the normal membrane trafficking pathway of the host cell, with this alteration possibly contributing toward more hospitable intracellular conditions for their growth and multiplication. Rab GTPases play pivotal roles in membrane trafficking (20,21). Therefore, the activity and localization of

these regulatory proteins may be targeted by intracellular pathogens to establish a niche for their proliferation (28). Several reports have investigated the localization of Rab5 and Rab7 on mycobacterial phagosomes (14–17,29,30), because Rab5 and Rab7 localize to the phagosome and co-ordinately contribute to the control of phagosome maturation (1). The localization of Rab14 and Rab22a on mycobacterial phagosomes was also shown to regulate early stages of phagosome maturation (12,19). However, little is known about how mycobacteria subvert the network of Rab GTPases regulating phagosome maturation within infected macrophages. In this study, we compared the subcellular localization of 42 distinct Rab GTPases on *M. tb*-containing phagosomes with that on *S. aureus*-containing phagosomes in macrophages to further understand how mycobacteria disrupt membrane trafficking in phagosomes.

We found that 22 Rab GTPases were recruited to *S. aureus*-containing phagosomes and that 17 of these Rab GTPases showed different localization kinetics on *M. tb*-containing phagosomes (Figure 2). We also found that some Rab GTPases localizing to phagosomes regulated phagosomal acidification and the recruitment of cathepsin D to the phagosome (Figures 4 and 5). This is the first report demonstrating that Rab20, Rab22b, Rab32, Rab34, Rab38, Rab39 and Rab43 regulate phagosome

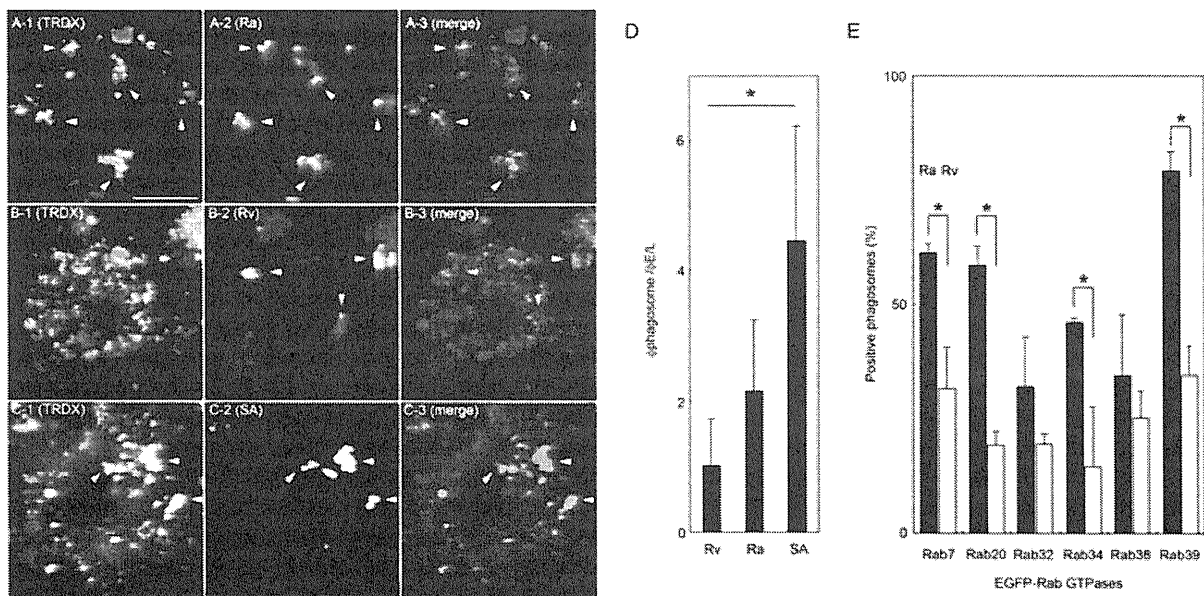


**Figure 7: Accession of lysosomes with the phagosomes correlates with phagosomal localization of Rab GTPases regulating phagosomal maturation.** A–C Raw264.7 macrophages preloaded with Texas Red-dextran were infected with (A) *M. tb* strain H37Ra (Ra), (B) *M. tb* strain H37Rv (Rv) and (C) *S. aureus* (SA) labeled with Alexa405-fluorophore for 6 h. Fixed cells were observed by LSCM. A-1, B-1 and C-1 show macrophages labeled with fluorescent dextran. A-2, B-2 and C-2 show bacteria labeled with Alexa405-fluorophore. A-3, B-3 and C-3 show the merged images of macrophages and bacteria. Arrows and arrowheads demonstrate phagosomes with and without fluorescent dextran-labeled lysosomal vesicles, respectively. Scale bar, 10  $\mu$ m. D) Ratiometric quantification of fluorescent dextran within the phagosomes relative to that of other E/L components. The ratio of fluorescent density within the phagosomes ( $\phi$ phagosome) relative to that of other E/L components ( $\phi$ E/L) was shown. Data represent the means and standard deviations of three independent experiments in which more than 100 phagosomes were examined for each condition. \* $p < 0.05$  (Tukey–Kramer multiple comparison test). E) Recruitment of Rab GTPases regulating phagosomal maturation of *M. tb* strains H37Ra (Ra) and H37Rv (Rv). Raw264.7 macrophages were transfected with plasmids encoding EGFP-fused Rab GTPases. Macrophages were infected with *M. tb* strains H37Ra or H37Rv labeled with Texas Red, fixed at 6 h (Rab7, Rab34 and Rab39), 1 h (Rab32 and Rab38) and 30 min (Rab20), and then observed by LSCM. Data represent the means and standard deviations of three independent experiments in which more than 100 phagosomes were counted for each condition. \* $p < 0.05$  (unpaired Student's *t*-test).

maturation. Rab22b, Rab32, Rab34 and Rab38 were reported to localize to the trans-Golgi network (31–33). We found that these Rab GTPases showed various association and dissociation kinetics with the phagosomes (Figure 2A) and were involved in the recruitment of cathepsin D to the phagosome. Our observations are consistent with a previous report showing the direct transport of cathepsin D from the trans-Golgi network to the phagosome (34). Rab34 is also reported to interact with RILP (32), suggesting its involvement in the promotion of phagolysosome biogenesis. In the present study, Rab43, a regulator of endoplasmic reticulum–Golgi trafficking (35), was also found to regulate the recruitment of cathepsin D to the phagosome. Rab20 was reported to localize to the endoplasmic reticulum (36) and colocalize with vacuolar-type ATPases (37). Additionally, we demonstrated the involvement of Rab20 in both phagosomal acidification and cathepsin D recruitment. We also found that Rab39 regulates phagosomal acidification and colocalizes with lysosomes (Table S1). Considering its recruitment kinetics to the phagosomes (Figure 2), Rab39 seems to maintain the phagosomal acidification at the late stage of phagocytosis. These observations, taken together, suggest that

these Rab GTPases differentially regulate phagosomal maturation at the various stages of phagocytosis.

Rab5 is widely accepted as a marker of mycobacterial phagosomes in infected macrophages (14,15). In this study, we found that Rab5 is not recruited to *M. tb*-containing phagosomes at 10 min p.i. (Figure 2). However, Kelley and Schorey (15) investigated Rab5 recruitment to the phagosomes containing *Mycobacterium avium* using a retrovirus transduction system. A previous live cell imaging analysis revealed that Rab5 is transiently associated with and then dissociated from mycobacterial phagosomes immediately after infection (12). We also found that Rab5 was recruited to approximately 40% of phagosomes containing *Mycobacterium bovis* strain bacille Calmette–Guérin (BCG) in Raw264.7 macrophages at 10 min p.i. (Figure S4). These results suggest that the kinetics of Rab5 recruitment to the phagosomes is different between the mycobacteria infected. Inconsistent with the fluorescent microscopic analysis, Rab5 could be detected in phagosomal fractions containing *M. tb* and latex beads by immunoblotting analysis at 6 h p.i. (Figures 2 and 3). Desjardins et al. (27) showed that recruited Rab5 to the

latex bead-containing phagosome decreases continuously over time. Via et al. (14) also reported that recruited Rab5 to the phagosomes containing latex beads or *M. bovis* BCG decreases over time but detectable by immunoblotting analysis. It is likely that the detection of Rab5 recruitment to the phagosomes at 6 h p.i. in our study is caused by the high sensitivity of immunoblotting analysis.

Rab7 localization on mycobacterial phagosomes has been controversial for a long time. Rab7 was reported to be absent from mycobacterial phagosomes in macrophages (12–15). Clemens et al. (29) reported that Rab7 localizes to *M. tb*-containing phagosomes in HeLa cells, but they also mentioned that Rab7 localization is caused by its overexpression. Sun et al. (16) demonstrated that Rab7 localizes to phagosomes containing *M. bovis* BCG in Raw264.7 macrophages. Recently, proteomic analysis also revealed that Rab7 localizes to the phagosomes containing *M. bovis* BCG in a human monocyte cell line (38). Rab7 depletion by RNA interference increased the proliferation of *Mycobacterium fortuitum* in *Drosophila* S2 cells (39), but did not affect proliferation of *M. tb* in a human monocyte cell line (40). These results suggest that Rab7 localizes to phagosomes containing avirulent mycobacteria, but not to those containing virulent mycobacteria, leading to inhibition of avirulent mycobacterial proliferation. Our previous and current studies demonstrated that Rab7 is transiently recruited to, and subsequently released from *M. tb*-containing phagosomes using imaging and immunoblotting analyses (Figures 2 and 3) (17). This dissociation would invalidate Rab7-mediated inhibition of *M. tb* proliferation in macrophages. We found that Rab20 shows a very weak localization to *M. tb*-containing phagosomes and regulates both phagosomal acidification and recruitment of cathepsin D (Figures 2, 4 and 5). The recruitment of Rab20 to *S. aureus*-containing phagosomes occurs transiently at 30 min after phagocytosis, when Rab7 recruitment coincides. We confirmed that the expression of Rab7DN and Rab20DN did not inhibit the recruitment of Rab20 and Rab7, respectively (data not shown), indicating that they independently contribute to phagosome maturation. Considering that Rab7 depletion inhibits the biogenesis of lysosomes (41), the function of Rab7 in the biogenesis of lysosomes has a significant connection to phagosome maturation and phagolysosome biogenesis. This finding raises the possibility that Rab20 contributes to phagosome maturation in other ways such as the biogenesis of late endosomes or lysosomes. Taken together, these results suggest that the dissociation of Rab7 and Rab20 from *M. tb*-containing phagosomes contributes to arresting the maturation of *M. tb*-containing phagosomes.

Transferrin receptors remain on mycobacterial phagosomes as a result of phagosomal fusion with early endosomal vesicles (42). In this study, we found that Rab11a and Rab11b are transiently recruited to *S. aureus*-containing phagosomes, but not *M. tb*-containing phagosomes (Figure 2). According to the evidence that Rab11 is

involved in the recycling of transferrin receptors (43), the failure to recruit Rab11a/b might be one of the reasons why transferrin receptors are associated with *M. tb*-containing phagosomes. Rab14 and Rab22a were reported to localize to mycobacterial phagosomes and arrest phagosome maturation (12,19). In this study, we found that these Rab GTPases were transiently recruited to *M. tb*-containing phagosomes through imaging and immunoblotting analyses (Figures 2 and 3). Our results also showed that Rab14 and Rab22a were recruited to *S. aureus*- and the latex bead-containing phagosomes (Figures 2 and 3), while other imaging analyses showed no localization of these Rab GTPases to latex bead or inactivated mycobacterial phagosomes (12,19). Certain proteomic analysis results support the association of these Rab GTPases with the latex bead-containing phagosomes (22–24). It is possible that the differing results between imaging and immunoblotting analyses of Rab14 and Rab22a recruitment to the latex-bead phagosome were caused by the emphasizing effect of our imaging analysis due to overexpression of GFP fusion proteins. We also found that the CA and DN forms of these Rab GTPases had no influence on the fusion of lysosomal vesicles with phagosomes containing *S. aureus* or *M. tb* (data not shown). These results suggest that Rab14 and Rab22a are passive markers for the progression of phagosome maturation.

Some Rab GTPases that were not recruited to phagosomes containing a virulent *M. tb* strain were actively associated with phagosomes containing the avirulent *M. tb* strain H37Ra (Figure 7E) or *M. bovis* BCG (data not shown). In parallel with the recruitment of Rab GTPases regulating phagosome maturation, the ability of *M. tb* H37Ra to inhibit phagolysosome biogenesis was weaker than that of *M. tb* H37Rv (Figure 7A–D). These findings raise the possibility that the recruitment of Rab GTPases to virulent *M. tb*-containing phagosomes is modulated. It is known that ESAT-6 secretion is inhibited in *M. tb* strain H37Ra (44), and that *M. bovis* BCG lacks the RD-1 region encoding genes for ESAT-6 and secretion machineries for ESAT-6 and other secretory proteins (ESX-1) (45). These observations suggest that virulence proteins secreted by ESX-1 directly or indirectly control the dissociation of Rab GTPases from *M. tb*-containing phagosomes. Of these virulent proteins, ESAT-6 may be involved in the dissociation of Rab GTPases from *M. tb*-containing phagosomes, as it is reported to induce pore formation on biomembranes (46). Pore formation in phagosomal membranes may cause the instability or dissociation of Rab GTPases anchoring to the phagosomes.

Cardoso et al. (47) reported that Rab10 regulates phagosome maturation and does not localize to phagosomes containing *M. bovis* BCG. They also reported that the expression of CA or DN forms of Rab10 modulates the maturation of mycobacterial phagosomes (47). We observed that about 10% of *S. aureus*-containing phagosomes, but less than 1% of *M. tb*-containing phagosomes acquire Rab10 at 10 min p.i. (Figure S4). We did not



examine the function of Rab10 in phagosome maturation in detail in this study because the association of Rab10 to the phagosome was very weak in our experimental system.

In conclusion, we propose a model in which the network of Rab GTPases regulates phagosome maturation, and the recruitment of Rab GTPases are modulated by phagosomes containing *M. tb* during inhibition of phagolysosome biogenesis (Figure S5). At least 22 Rab GTPases localize on the phagosome transiently or consecutively during progression of phagosome maturation, with Rab7, Rab20 and Rab39 regulating acidification of the phagosome. Rab7, Rab20, Rab22b, Rab32, Rab34, Rab38 and Rab43 regulate the recruitment of cathepsin D to the phagosome. The recruitment of these Rab GTPases to *M. tb*-containing phagosomes is modulated, except for Rab22b and Rab43. The current study does not support that *M. tb* directly targets these Rab GTPases during *M. tb*-induced inhibition of phagolysosome biogenesis, but suggests that the modulation of the recruitment of Rab GTPases to *M. tb*-containing phagosomes is involved in the arrest of phagosome maturation and inhibition of phagolysosome biogenesis. We are currently investigating the roles of these Rab GTPases in phagolysosome biogenesis to further understand how *M. tb* evades killing activities within the phagosome.

## Materials and Methods

### Cell and bacterial cultures

Raw264.7 macrophages were obtained from the American Type Culture Collection and maintained in DMEM (Sigma-Aldrich) supplemented with 10% FBS (Invitrogen), 25 µg/mL penicillin G and 25 µg/mL streptomycin, at 37°C under 5% CO<sub>2</sub>. *M. tb* strains, H37Rv and H37Ra, were obtained from Japan Research Institute of Tuberculosis. *M. bovis* BCG Tokyo was obtained from Japan BCG Laboratory. *M. tb* strains H37Rv and H37Ra, and *M. bovis* BCG, were grown to mid-logarithmic phase in 7H9 medium supplemented with 10% Middlebrook ADC (BD Biosciences), 0.5% glycerol and 0.05% Tween 80 (*Mycobacterium* complete medium) at 37°C. *M. tb* transformed with a plasmid encoding DsRed (48) was grown in *Mycobacterium* complete medium containing 25 µg/mL kanamycin. *S. aureus* was grown in brain heart infusion broth (BD Biosciences) at 37°C.

### Bacteria labeling

*M. tb* and *S. aureus* were labeled with Texas Red or Alexa405 (Invitrogen) as described previously (49), with minor modifications. Briefly, bacterial cultures were centrifuged for 5 min at 8000 × *g* and washed with PBS three times. Bacterial cells were then labeled with 20 µg/mL Texas Red ester or 100 µg/mL Alexa405 succinimidyl ester in PBS at 37°C for 30 min, followed by washing with PBS containing 0.05% Tween 80 for mycobacteria and PBS for *S. aureus*. Labeled bacteria were then suspended in DMEM with 10% FBS and incubated at 37°C for 30 min. Bacterial suspensions were passed through a 26-gauge needle 10 times and centrifuged for 5 min at 1000 × *g* to remove clumps and aggregates. If necessary, *M. tb* was heat inactivated before labeling with fluorescent dyes by incubation at 90°C for 10 min. The viability of heat-inactivated *M. tb* cells were confirmed as less than 1% of that of nontreated bacteria by a colony counting assay. *M. tb* expressing DsRed was washed three times with PBS containing 0.05% Tween 80, and then a single cell suspension was prepared. The viability of inoculated bacteria labeled with fluorescent dyes or expressing DsRed was confirmed more than 99% by staining with SYTOX Green (Invitrogen).

### Infection of bacteria

Transfected cells grown on round coverslips in 12-well plates were infected with bacteria. Bacterial cells were washed with PBS containing 0.05% Tween 80 three times and suspended in DMEM with 10% FBS at a multiplicity of infection (MOI) of 10–30. Aliquots of 1 mL of bacterial suspension were added to 3 × 10<sup>5</sup> cells of Raw264.7 macrophages on coverslips in 12-well plates, followed by centrifugation at 150 × *g* for 5 min and incubation for 10 min at 37°C. Infected cells on coverslips were washed with DMEM three times to remove non-phagocytosed bacteria and then incubated with DMEM containing 10% FBS. At the indicated time-points, infected cells were fixed with 1 or 3% paraformaldehyde in PBS.

### Antibodies

Rabbit anti-Rab5 polyclonal antibody (Abcam), mouse anti-Rab7 monoclonal antibody (Abcam), rabbit anti-Rab9 monoclonal antibody (Abcam), rabbit anti-Rab14 polyclonal antibody (Sigma-Aldrich), rabbit anti-Rab22a polyclonal antibody (Proteintech Group, Inc.), rat anti-mouse LAMP-2 monoclonal antibody (SouthernBiotech) and goat anti-mouse cathepsin D polyclonal antibody (R&D systems) were all purchased. Alexa488- and Alexa546-anti-IgG antibodies (Invitrogen) were purchased.

### Isolation of the latex bead- and *M. tb*-containing phagosomes

Eight 15-cm plates of Raw264.7 macrophages were used for each condition. For isolation of latex-bead phagosomal fractions, latex beads (0.7 µm, Polysciences, Inc.) were added to cells for 2 h, washed three times with prewarmed DMEM. For preparation of 2- or 8-h phagosomal fractions, cells were collected immediately after washing or further incubated in DMEM with 10% FBS, respectively. Collected cells were lysed and subjected to discontinuous sucrose gradient centrifugation as described previously (27). For isolation of *M. tb* phagosomal fractions, bacteria at an MOI of 30 were infected to Raw264.7 for 2 h, washed and then incubated for the indicated times. Infected cells were collected, lysed and subjected to fractionation as described previously (26). Both phagosomal fractions were extracted by the cell lysis buffer containing 25 mM Tris-HCl pH 7.6, 150 mM NaCl, 1% Nonidet P-40, 1% sodium deoxycholate and 0.1% SDS. We confirmed that mycobacterial proteins are not extracted by the cell lysis buffer as described previously (38). For immunoblotting analysis, aliquots of 50 µg of Raw264.7 cell lysate and 6 µg of phagosomal fractions were separated by SDS-PAGE and then subjected to immunoblotting analysis using anti-Rab5 antibody (1:100 v/v), anti-Rab7 antibody (1:100 v/v), anti-Rab9 (1:100 v/v), anti-Rab14 (1:100 v/v) and anti-Rab22a (1:100 v/v). Band intensity from three independent experiments was quantified by IMAGEJ (<http://rsbweb.nih.gov/ij/>).

### Thin-section electron microscopy

Phagosomal fractions were isolated at 6 h p.i., fixed with 1% glutaraldehyde in 0.1 M sodium phosphate buffer (pH 7.4) and washed with phosphate buffer. Fixed phagosomal fractions were incubated with 0.1% (w/v) osmium tetroxide. Dehydration was carried out with a series of ethanol washes, followed by treatment with propylene oxide. Samples were embedded in Qetol812 resin (OKEN) according to the manufacturer's protocol. Thin sections were cut with diamond knives and mounted on copper grids. Sections on grids were counter stained with 2% (w/v) uranyl acetate and then observed with a JEM-1220 electron microscope (JEOL).

### LysoTracker staining, labeling lysosomal vesicles with fluorescent dextran and immunofluorescence microscopy

For LysoTracker staining, cells were incubated with 300 nm LysoTracker Red DND-99 (Invitrogen) for 30 min before fixation. Stained cells were fixed with 1% paraformaldehyde in PBS for 1 h, washed with PBS and observed by LSCM as previously described (17). For flow cytometric analysis, macrophages stained with LysoTracker were washed with PBS and suspended in PBS containing 1% FBS. Flow cytometric analysis was performed on a FACSAria flow cytometer (BD Bioscience). For

## Localization of Rab GTPases on *M. tb*-Containing Phagosomes

labeling lysosomal vesicles with fluorescent dextran, cells were incubated with Texas Red-dextran (Invitrogen) at 100 µg/mL for 8 h, followed by washing and chasing in fluorescent-dextran-free DMEM with 10% FBS for 16 h. Immunofluorescence microscopy was performed as previously described (17). For quantification of fluorescence, serial confocal sections at 0.5 µm steps within a z-stack spanning a total thickness of 12 µm were taken, and z-stacks were collapsed into a single x–y projection. The accumulation of LysoTracker, cathepsin D and fluorescent dextran within the phagosome and other E/L components was quantified by IMAGEJ using collapsed fluorescent images. Fluorescent density was calculated as that the fluorescent intensity is divided by the area.

### Plasmid constructs and transfection

PCR was carried out using cDNA derived from HeLa cells as a template and the primer sets were listed in Table S2. PCR products of the amplified Rab GTPase genes were inserted into the pEGFP-C1 (Invitrogen) or pCI (Promega) vectors. CA and DN mutants of Rab GTPases were prepared by site-directed mutagenesis as described previously (50,51) using the primer sets listed in Table S3. Transfection of cells with plasmid was performed as described previously (17). Briefly, two million cells of Raw264.7 macrophages were transfected with 10 µg of plasmid DNA using an MP-100 electroporator (Digital Bio Technology), according to the manufacturer's instructions. Transfected cells were incubated in DMEM with 10% FBS for 24 h prior to the experiments.

### Statistics

The unpaired or paired two-sided Student's *t*-test was used to assess the statistical significance of differences between the two groups. Tukey–Kramer multiple comparison test was used for the assessment of the statistical significance of differences among three groups. For the assessment of the differences of the proportions of fluorescence-positive phagosomes, we did three independent experiments and counted more than 100 phagosomes at each condition. Assessment of the differences in fluorescent density accumulating within the phagosomes was conducted over three independent experiments, with more than 100 phagosomes examined for each condition.

## Acknowledgments

We thank Drs Toshi Nagata and Masato Uchijima (Hamamatsu University School of Medicine, Hamamatsu, Japan) for their helpful discussions. We also thank Ms Yumiko Suzuki (Hamamatsu University School of Medicine) for her excellent assistance. This work was supported in part by Grants-in-Aid for Young Scientists (B), Scientific Research (B) and Scientific Research (C) from the Japan Society for the Promotion of Science; Scientific Research on Priority Areas from the Ministry of Education, Culture, Sports, Science and Technology of Japan; the Health and Labour Science Research Grants for Research into Emerging and Reemerging Infectious Diseases from the Ministry of Health, Labour and Welfare of Japan and the United States–Japan Cooperative Medical Science Committee.

## Supporting Information

Additional Supporting Information may be found in the online version of this article:

**Figure S1: Localization of Rab GTPases on *S. aureus*- and *M. tb*-containing phagosomes.** The subcellular localization of the Rab GTPases from Figure 2 is shown. Raw264.7 macrophages expressing EGFP-Rab GTPases were infected with *S. aureus* labeled with Texas Red (SA) or *M. tb* expressing DsRed (MTB). Infected cells were fixed at the indicated time-points and observed by LSCM. Left and right panels show images of macrophages with and without images of infected bacteria, respectively. Arrows and arrowheads indicate phagosomes with and without the localization of Rab GTPases, respectively. Scale bar, 10 µm.

**Figure S2: Rab GTPases not associated with *S. aureus*-containing phagosomes.** The subcellular localization of 20 Rab GTPases are shown. No significant associations with *S. aureus* (A) and *M. tb* (B) were observed at any of the time-points up to 6 h (less than 20% of the phagosomes).

**Figure S3: Flow cytometric analysis reveals that expression of the DN forms of Rab GTPases has no influence on the generation of acidic vesicles in macrophages.** Macrophages were transfected with expression plasmids for EGFP and the DN forms of Rab GTPases. Transfected cells were stained with 300 nm LysoTracker for 30 min, followed by flow cytometric analysis. The ratio of mean fluorescent intensity derived from GFP-positive cells (Q2) to that from GFP-negative cells (Q4) is indicated. The proportions of cells that were GFP positive (Q2) and negative (Q4) are also indicated.

**Figure S4: Localization of Rab5 and Rab10 to the phagosomes.** A) Raw264.7 macrophages expressing EGFP-Rab5 were infected with *M. bovis* BCG. B and C) Raw264.7 macrophages expressing EGFP-Rab10 were infected with *S. aureus* (SA) or *M. tb* (MTB). A-1, B-1 and C-1 show subcellular localization of Rab GTPases (Rab5 and Rab10). A-2, B-2 and B-3 show bacteria (BCG, SA and MTB). A-3, B-3 and C-3 show the merged images of macrophage and bacteria (merge). Arrows and arrowheads indicate phagosomes with and without the localization of Rab GTPases, respectively. Scale bar, 10 µm.

**Figure S5: Rab GTPases recruited to phagosomes containing *M. tb*.** Rab GTPases recruited to phagosomes containing *S. aureus* or *M. tb* are shown. Rab GTPases shown in blue, green or red are involved in phagosomal acidification, cathepsin D recruitment to the phagosomes or both, respectively. Boxed Rab GTPases are dissociated from *M. tb*-containing phagosomes. EE, early endosomes; ER, endoplasmic reticulum; LE, late endosomes; LY, lysosomes; RE, recycling endosomes; TGN, trans-Golgi network.

**Table S1:** Subcellular localization of Rab GTPases

**Table S2:** Primer list for construction of plasmid of EGFP-fused Rab GTPases

**Table S3:** Primer list for site-directed mutagenesis

Please note: Wiley-Blackwell are not responsible for the content or functionality of any supporting materials supplied by the authors. Any queries (other than missing material) should be directed to the corresponding author for the article.

## References

1. Vieira OV, Botelho RJ, Grinstein S. Phagosome maturation: aging gracefully. *Biochem J* 2002;366:689–704.
2. Vieira OV, Botelho RJ, Rameh L, Brachmann SM, Matsuo T, Davidson HW, Schreiber A, Backer JM, Cantley LC, Grinstein S. Distinct roles of class I and class III phosphatidylinositol 3-kinases in phagosome formation and maturation. *J Cell Biol* 2001;155:19–25.
3. Kitano M, Nakaya M, Nakamura T, Nagata S, Matsuda M. Imaging of Rab5 activity identifies essential regulators for phagosome maturation. *Nature* 2008;453:241–245.
4. Vieira OV, Bucci C, Harrison RE, Trimble WS, Lanzetti L, Gruenberg J, Schreiber AD, Stahl PD, Grinstein S. Modulation of Rab5 and Rab7 recruitment to phagosomes by phosphatidylinositol 3-kinase. *Mol Cell Biol* 2003;23:2501–2514.
5. Harrison RE, Bucci C, Vieira OV, Schroer TA, Grinstein S. Phagosomes fuse with late endosomes and/or lysosomes by extension of membrane protrusions along microtubules: role of Rab7 and RILP. *Mol Cell Biol* 2003;23:6494–6506.
6. Armstrong JA, Hart PD. Response of cultured macrophages to *Mycobacterium tuberculosis*, with observations on fusion of lysosomes with phagosomes. *J Exp Med* 1971;134:713–740.
7. Clemens DL, Horwitz MA. Characterization of the *Mycobacterium tuberculosis* phagosome and evidence that phagosomal maturation is inhibited. *J Exp Med* 1995;181:257–270.

8. Russell DG. *Mycobacterium tuberculosis*: here today, and here tomorrow. *Nat Rev Mol Cell Biol* 2001;2:569–577.
9. Rink J, Ghigo E, Kalaidzidis Y, Zerial M. Rab conversion as a mechanism of progression from early to late endosomes. *Cell* 2005;122:735–749.
10. Vergne I, Chua J, Singh SB, Deretic V. Cell biology of *Mycobacterium tuberculosis* phagosome. *Annu Rev Cell Dev Biol* 2004;20:367–394.
11. Deretic V, Vergne I, Chua J, Master S, Singh SB, Fazio JA, Kyei G. Endosomal membrane traffic: convergence point targeted by *Mycobacterium tuberculosis* and HIV. *Cell Microbiol* 2004;6:999–1009.
12. Roberts EA, Chua J, Kyei GB, Deretic V. Higher order Rab programming in phagolysosome biogenesis. *J Cell Biol* 2006;174:923–929.
13. Vergne I, Chua J, Lee HH, Lucas M, Belisle J, Deretic V. Mechanism of phagolysosome biogenesis block by viable *Mycobacterium tuberculosis*. *Proc Natl Acad Sci U S A* 2005;102:4033–4038.
14. Via LE, Deretic D, Ulmer RJ, Hibler NS, Huber LA, Deretic V. Arrest of mycobacterial phagosome maturation is caused by a block in vesicle fusion between stages controlled by rab5 and rab7. *J Biol Chem* 1997;272:13326–13331.
15. Kelley VA, Schorey JS. *Mycobacterium*'s arrest of phagosome maturation in macrophages requires Rab5 activity and accessibility to iron. *Mol Biol Cell* 2003;14:3366–3377.
16. Sun J, Deghmane AE, Soualhine H, Hong T, Bucci C, Solodkin A, Hmama Z. *Mycobacterium bovis* BCG disrupts the interaction of Rab7 with RILP contributing to inhibition of phagosome maturation. *J Leukoc Biol* 2007;82:1437–1445.
17. Seto S, Matsumoto S, Ohta I, Tsujimura K, Koide Y. Dissection of Rab7 localization on *Mycobacterium tuberculosis* phagosome. *Biochem Biophys Res Commun* 2009;387:272–277.
18. Seto S, Matsumoto S, Tsujimura K, Koide Y. Differential recruitment of CD63 and Rab7-interacting-lysosomal-protein to phagosomes containing *Mycobacterium tuberculosis* in macrophages. *Microbiol Immunol* 2010;54:170–174.
19. Kyei GB, Vergne I, Chua J, Roberts E, Harris J, Junutula JR, Deretic V. Rab14 is critical for maintenance of *Mycobacterium tuberculosis* phagosome maturation arrest. *EMBO J* 2006;25:5250–5259.
20. Schwartz SL, Cao C, Pylpenko O, Rak A, Wandinger-Ness A. Rab GTPases at a glance. *J Cell Sci* 2007;120:3905–3910.
21. Stenmark H, Olkkonen VM. The Rab GTPase family. *Genome Biol* 2001;2:REVIEWS3007.
22. Garin J, Diez R, Kieffer S, Dermine JF, Duclos S, Gagnon E, Sadoul R, Rondeau C, Desjardins M. The phagosome proteome: insight into phagosome functions. *J Cell Biol* 2001;152:165–180.
23. Rogers LD, Foster LJ. The dynamic phagosomal proteome and the contribution of the endoplasmic reticulum. *Proc Natl Acad Sci U S A* 2007;104:18520–18525.
24. Shui W, Sheu L, Liu J, Smart B, Petzold CJ, Hsieh TY, Pitcher A, Keasling JD, Bertozzi CR. Membrane proteomics of phagosomes suggests a connection to autophagy. *Proc Natl Acad Sci U S A* 2008;105:16952–16957.
25. Smith AC, Heo WD, Braun V, Jiang X, Macrae C, Casanova JE, Scidmore MA, Grinstein S, Meyer T, Brumell JH. A network of Rab GTPases controls phagosome maturation and is modulated by *Salmonella enterica* serovar Typhimurium. *J Cell Biol* 2007;176:263–268.
26. Beatty WL, Rhoades ER, Hsu DK, Liu FT, Russell DG. Association of a macrophage galactoside-binding protein with *Mycobacterium*-containing phagosomes. *Cell Microbiol* 2002;4:167–176.
27. Desjardins M, Huber LA, Parton RG, Griffiths G. Biogenesis of phagolysosomes proceeds through a sequential series of interactions with the endocytic apparatus. *J Cell Biol* 1994;124:677–688.
28. Brumell JH, Scidmore MA. Manipulation of rab GTPase function by intracellular bacterial pathogens. *Microbiol Mol Biol Rev* 2007;71:636–652.
29. Clemens DL, Lee BY, Horwitz MA. *Mycobacterium tuberculosis* and *Legionella pneumophila* phagosomes exhibit arrested maturation despite acquisition of Rab7. *Infect Immun* 2000;68:5154–5166.
30. Fratti RA, Backer JM, Gruenberg J, Corvera S, Deretic V. Role of phosphatidylinositol 3-kinase and Rab5 effectors in phagosomal biogenesis and mycobacterial phagosome maturation arrest. *J Cell Biol* 2001;154:631–644.
31. Ng EL, Wang Y, Tang BL. Rab22B's role in trans-Golgi network membrane dynamics. *Biochem Biophys Res Commun* 2007;361:751–757.
32. Wang T, Hong W. Interorganellar regulation of lysosome positioning by the Golgi apparatus through Rab34 interaction with Rab-interacting lysosomal protein. *Mol Biol Cell* 2002;13:4317–4332.
33. Wasmeier C, Romao M, Plowright L, Bennett DC, Raposo G, Seabra MC. Rab38 and Rab32 control post-Golgi trafficking of melanogenic enzymes. *J Cell Biol* 2006;175:271–281.
34. Ullrich HJ, Beatty WL, Russell DG. Direct delivery of procathepsin D to phagosomes: implications for phagosome biogenesis and parasitism by *Mycobacterium*. *Eur J Cell Biol* 1999;78:739–748.
35. Dejgaard SY, Murshid A, Erman A, Kizilay O, Verbich D, Lodge R, Dejgaard K, Ly-Hartig TB, Pepperkok R, Simpson JC, Presley JF. Rab18 and Rab43 have key roles in ER-Golgi trafficking. *J Cell Sci* 2008;121:2768–2781.
36. Das Sarma J, Kaplan BE, Willemsen D, Koval M. Identification of rab20 as a potential regulator of connexin 43 trafficking. *Cell Commun Adhes* 2008;15:65–74.
37. Curtis LM, Gluck S. Distribution of Rab GTPases in mouse kidney and comparison with vacuolar H<sup>+</sup>-ATPase. *Nephron Physiol* 2005;100:31–42.
38. Lee BY, Jethwaney D, Schilling B, Clemens DL, Gibson BW, Horwitz MA. The *Mycobacterium bovis* bacille Calmette-Guerin phagosome proteome. *Mol Cell Proteomics* 2010;9:32–53.
39. Philips JA, Porto MC, Wang H, Rubin EJ, Perrimon N. ESCRT factors restrict mycobacterial growth. *Proc Natl Acad Sci U S A* 2008;105:3070–3075.
40. Kumar D, Nath L, Kamal MA, Varshney A, Jain A, Singh S, Rao KV. Genome-wide analysis of the host intracellular network that regulates survival of *Mycobacterium tuberculosis*. *Cell* 2010;140:731–743.
41. Vanlandingham PA, Ceresa BP. Rab7 regulates late endocytic trafficking downstream of multivesicular body biogenesis and cargo sequestration. *J Biol Chem* 2009;284:12110–12124.
42. Vergne I, Fratti RA, Hill PJ, Chua J, Belisle J, Deretic V. *Mycobacterium tuberculosis* phagosome maturation arrest: mycobacterial phosphatidylinositol analog phosphatidylinositol mannoside stimulates early endosomal fusion. *Mol Biol Cell* 2004;15:751–760.
43. Cox D, Lee DJ, Dale BM, Calafat J, Greenberg S. A Rab11-containing rapidly recycling compartment in macrophages that promotes phagocytosis. *Proc Natl Acad Sci U S A* 2000;97:680–685.
44. Frigui W, Bottai D, Majlessi L, Monot M, Josselin E, Brodin P, Garnier T, Gicquel B, Martin C, Leclerc C, Cole ST, Brosch R. Control of *M. tuberculosis* ESAT-6 secretion and specific T cell recognition by PhoP. *PLoS Pathog* 2008;4:e33.
45. Abdallah AM, Gey van Pittius NC, Champion PA, Cox J, Luirink J, Vandenbroucke-Grauls CM, Appelmek BJ, Bitter W. Type VII secretion – mycobacteria show the way. *Nat Rev Microbiol* 2007;5:883–891.
46. Smith J, Manoranjan J, Pan M, Bohsali A, Xu J, Liu J, McDonald KL, Szyk A, LaRonde-LeBlanc N, Gao LY. Evidence for pore formation in host cell membranes by ESX-1-secreted ESAT-6 and its role in *Mycobacterium marinum* escape from the vacuole. *Infect Immun* 2008;76:5478–5487.
47. Cardoso CM, Jordao L, Vieira OV. Rab10 regulates phagosome maturation and its overexpression rescues *Mycobacterium*-containing phagosomes maturation. *Traffic* 2010;11:221–235.
48. Aoki K, Matsumoto S, Hirayama Y, Wada T, Ozeki Y, Niki M, Domenech P, Umemori K, Yamamoto S, Mineda A, Matsumoto M, Kobayashi K. Extracellular mycobacterial DNA-binding protein 1 participates in mycobacterium-lung epithelial cell interaction through hyaluronic acid. *J Biol Chem* 2004;279:39798–39806.
49. Chua J, Deretic V. *Mycobacterium tuberculosis* reprograms waves of phosphatidylinositol 3-phosphate on phagosomal organelles. *J Biol Chem* 2004;279:36982–36992.
50. Fukuda M, Kanno E, Ishibashi K, Itoh T. Large scale screening for novel rab effectors reveals unexpected broad Rab binding specificity. *Mol Cell Proteomics* 2008;7:1031–1042.
51. Itoh T, Satoh M, Kanno E, Fukuda M. Screening for target Rabs of TBC (Tre-2/Bub2/Cdc16) domain-containing proteins based on their Rab-binding activity. *Genes Cells* 2006;11:1023–1037.

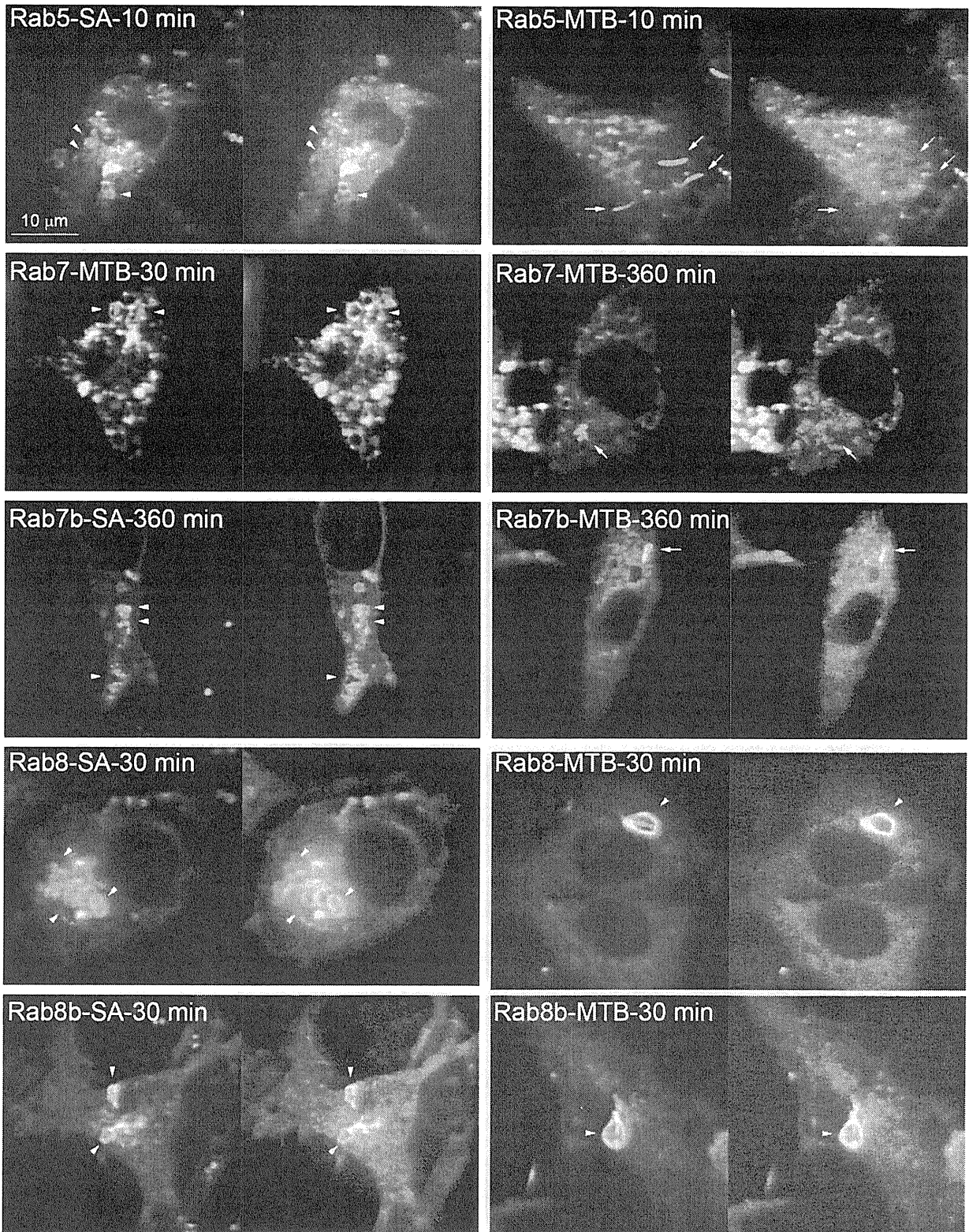


Figure S1-1

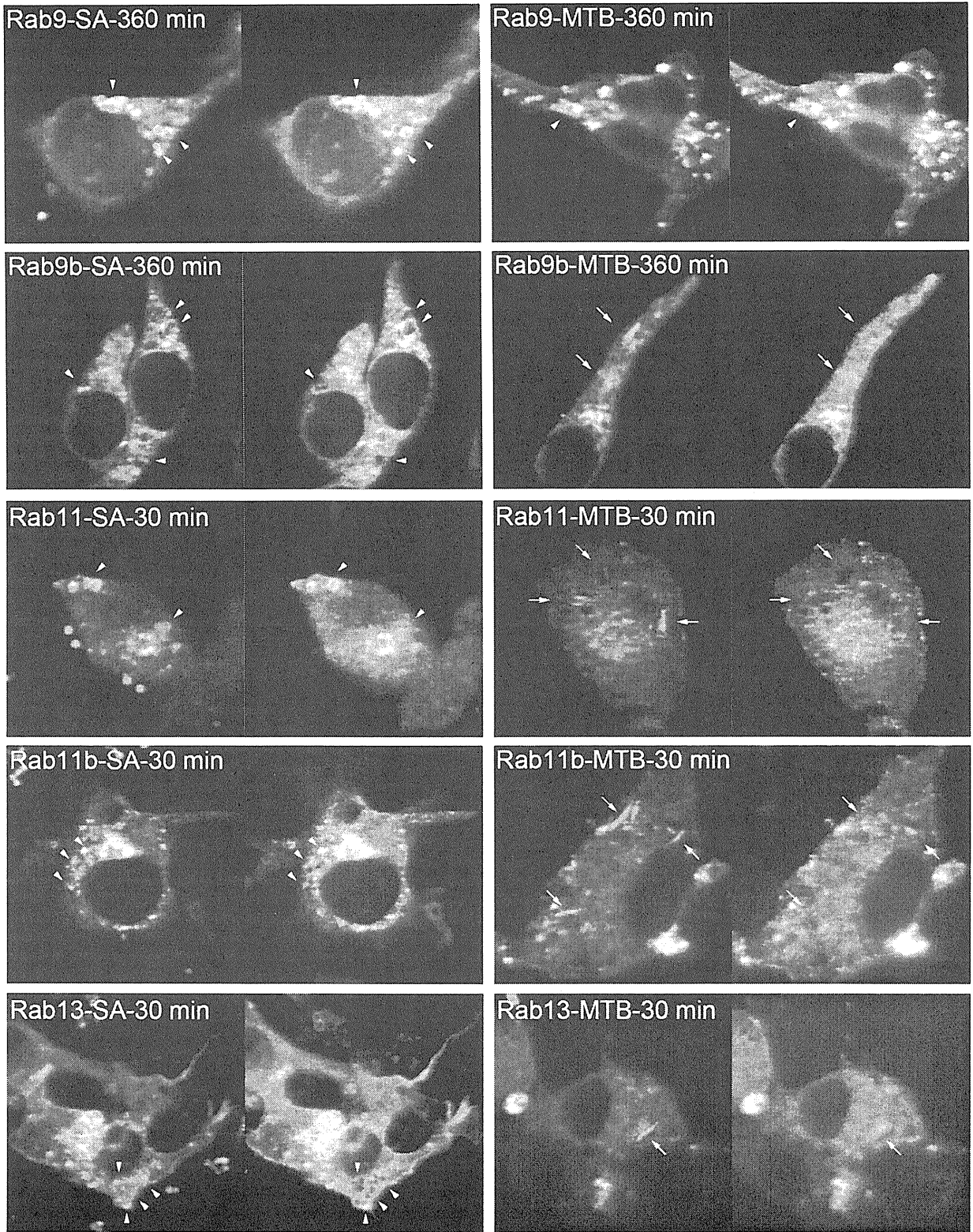


Figure S1-2

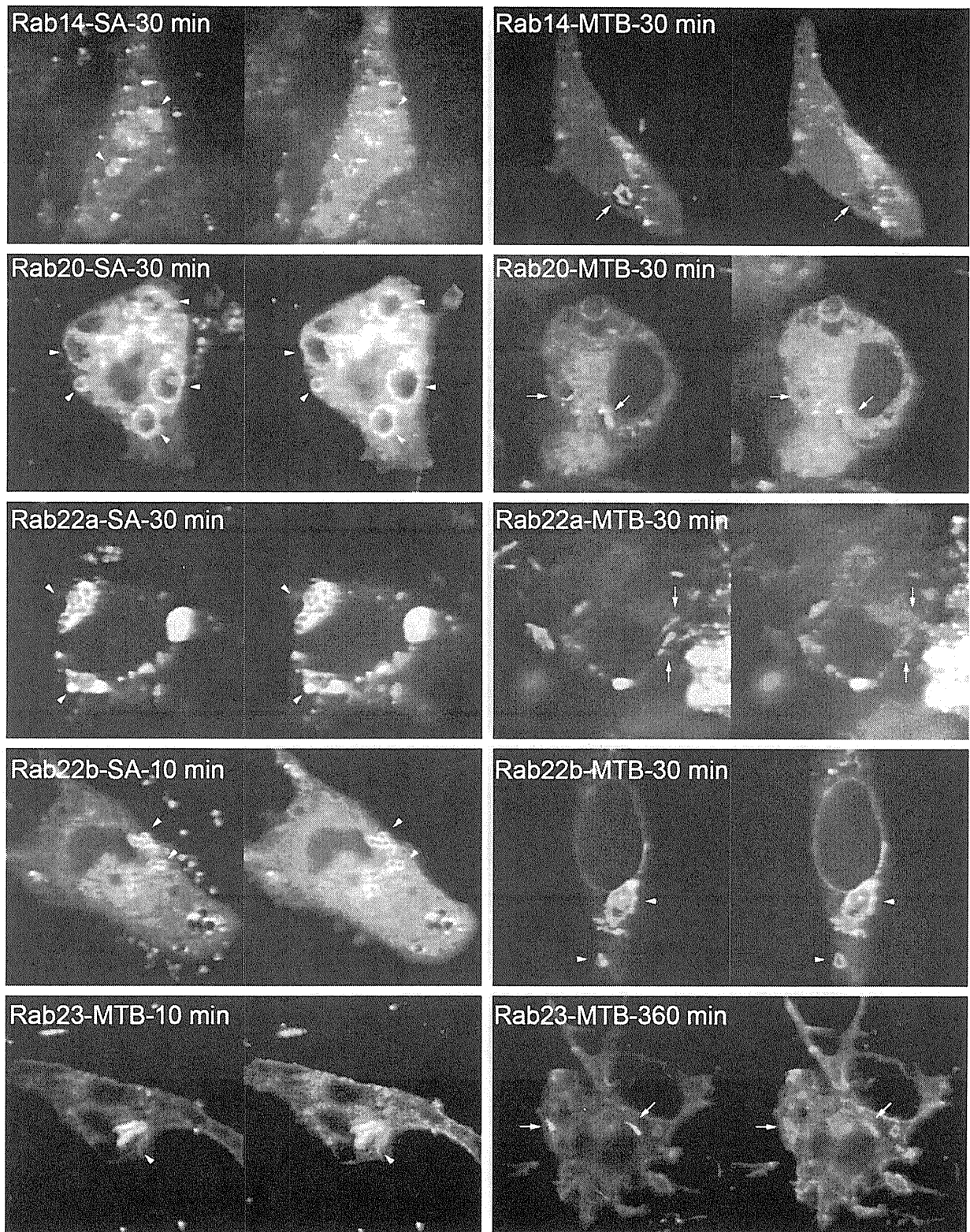


Figure S1-3

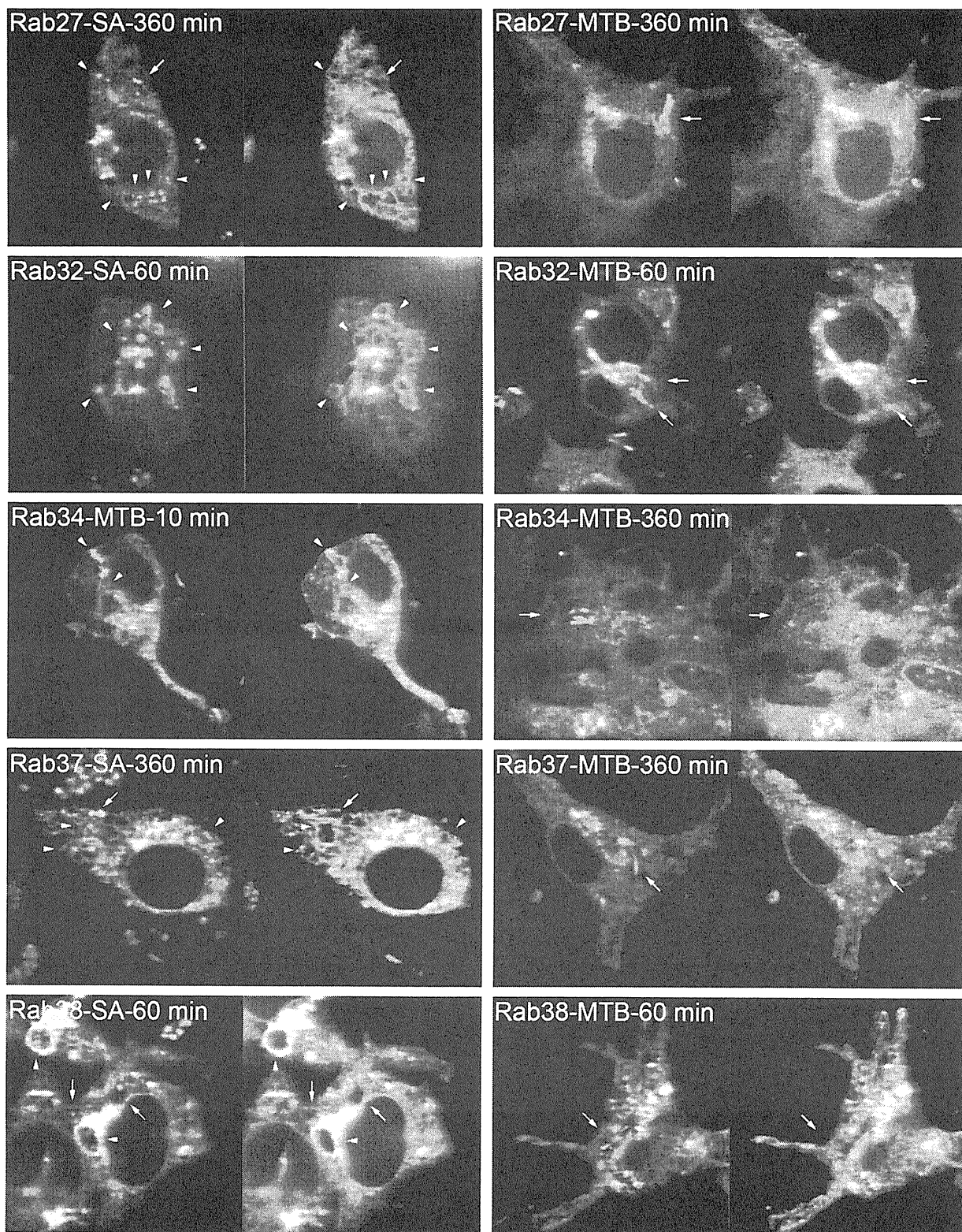


Figure S1-4

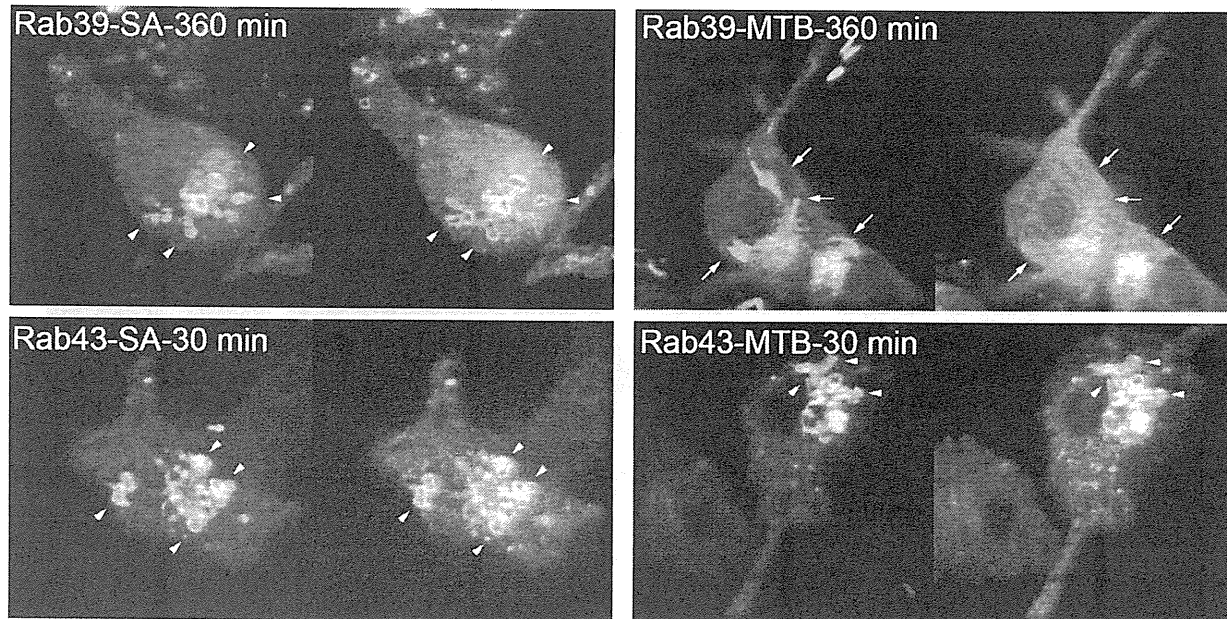


Figure S1-5



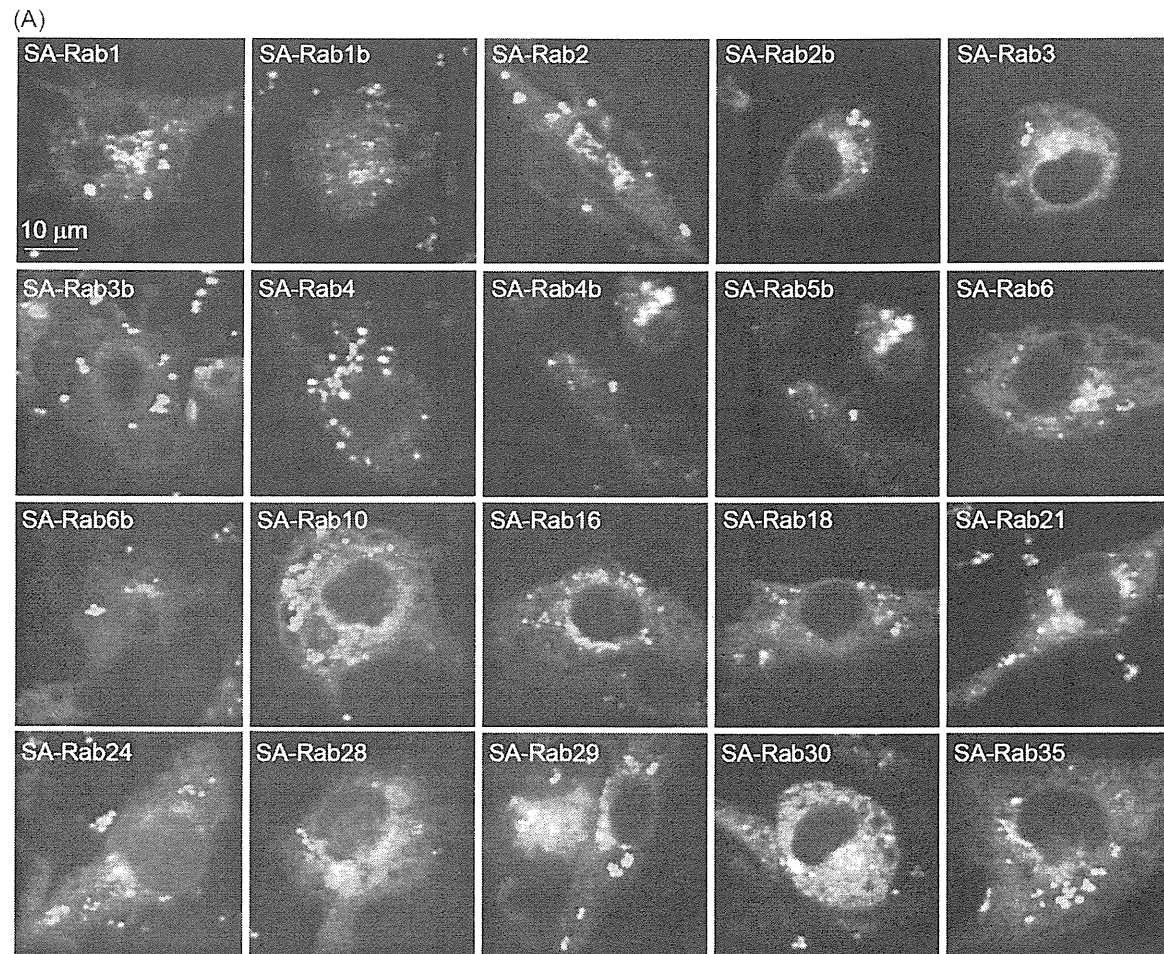


Figure S2A

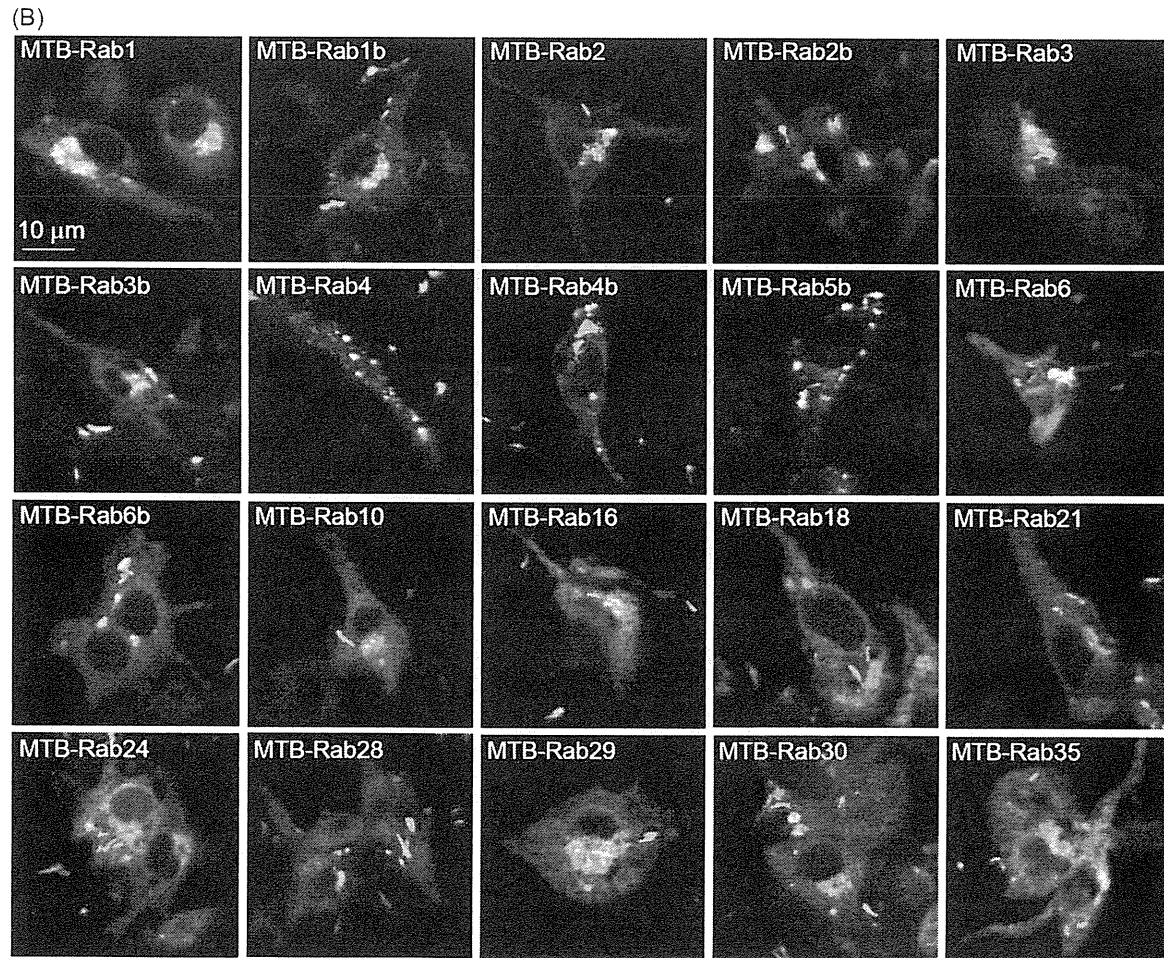


Figure S2B

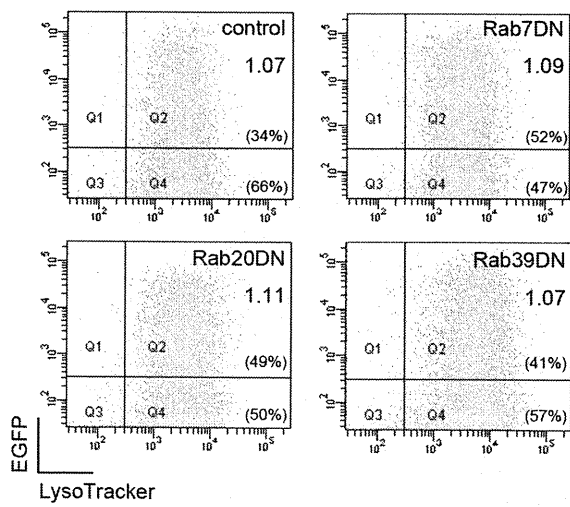


Figure S3

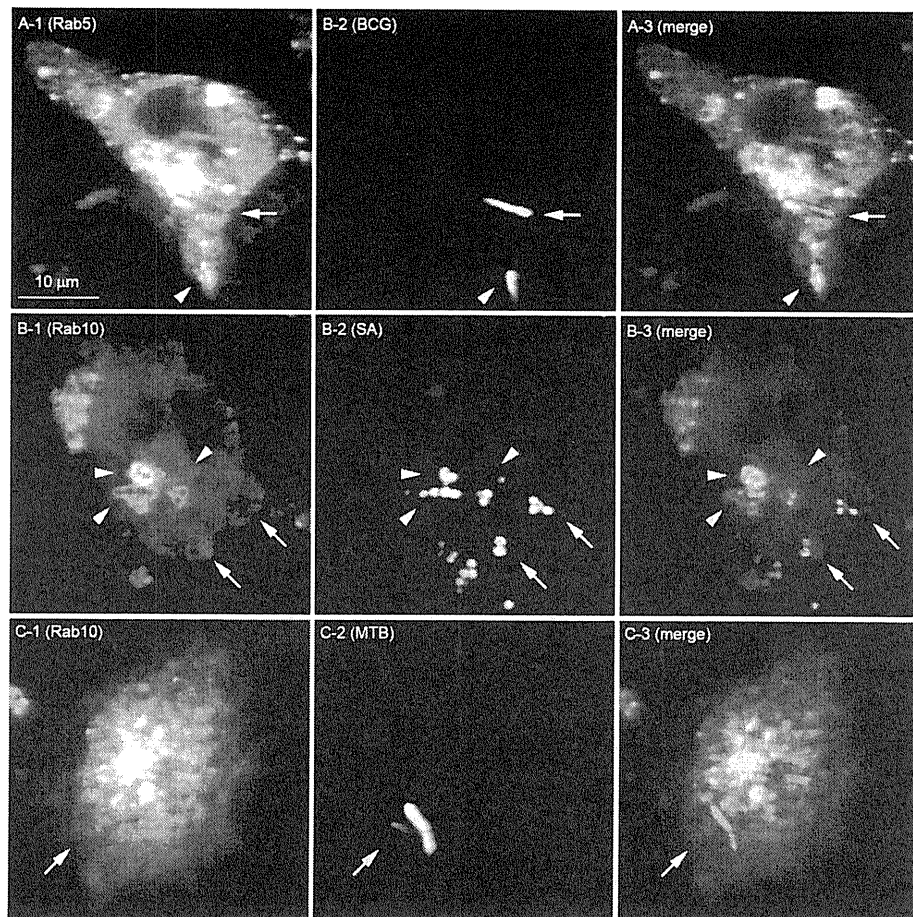


Figure S4